

STIFFNESS DAMAGE AND MECHANICAL TESTING OF CORE SPECIMENS FOR THE EVALUATION OF STRUCTURES AFFECTED BY ASR

Eric R. Giannini ^{1*}, Kevin J. Folliard¹

¹The University of Texas at Austin, Austin, TX, USA

Abstract

Mechanical tests of concrete core samples are an important component of evaluating concrete structures affected by alkali-silica reaction. Prior research suggests that the stiffness damage test may provide data that correlates linearly with the amount of expansion to-date, although this correlation must be established for a particular reactive aggregate. The test involves relatively low (10 MPa) compressive loads, which allow elastic modulus and compressive strength test to be conducted on the same cores. In this study, the stiffness damage test is performed on a concrete cores and cylinders at multiple expansion levels. Two test parameters were examined with the objective of establishing a linear correlation to expansion. Four reactive aggregates from the southwestern United States were investigated. The elastic modulus and compressive strength of the specimens were also measured.

Keywords: compressive strength, elastic modulus, existing structures, stiffness damage test, test methods

1 INTRODUCTION

Obtaining a reasonable estimate of expansion to date remains a challenging issue in the evaluation of structures affected by alkali-silica reaction (ASR). This information is valuable both in the assessment of the current effects of ASR on a structure, including the stresses in the reinforcement, as well as producing a prognosis for potential future expansion. ASR also results in the degradation of concrete's mechanical properties. Elastic modulus, tensile and flexural strengths are most affected; severe cases may reduce the elastic modulus by up to 70% [1,2,3]. Compressive strength has also been reported to decrease up to 40% in severe cases [1]. Although the strength and stiffness of concrete cores have yet to serve as a reliable predictor of structural performance [3], it is desirable to extract as much information as possible from each specimen.

Estimates obtained with surface crack width summation methods are valuable in the early stages of an investigation, but can be influenced by environmental conditions and operator judgement of crack widths, as well as forms of degradation other than expansion due to ASR [3]. Thus, they may provide insight into the order-of-magnitude of distress, but may still significantly over- or underestimate the actual expansion.

Quantitative petrography, such as the Damage Rating Index (DRI) method, has also been used to determine the order-of-magnitude of distress based on the identification of characteristic petrographic features of ASR on polished sections of core samples [4]. The method is extremely operator-dependant and concrete made with different reactive aggregates can produce vastly different DRI scores for a given amount of expansion [5,6]. Petrography is an essential step in diagnosing the presence of ASR, but can not provide information about the mechanical properties of concrete in the structure.

The stiffness damage test (SDT) has been identified as a potentially useful method of estimating expansion to date by applying cyclic loads to core specimens. Since the test is non-destructive, investigators

* Correspondence to: eric.giannini@mail.utexas.edu

are also free to conduct standard elastic modulus and compressive strength tests. Following compression testing, chemical tests (e.g. water- and acid-soluble alkalis, pore solution extraction) can be performed on the same specimens. As originally developed by Crouch and Wood, the test involved applying five cycles of 5.5 MPa compressive load to a core specimen and measuring the stress-strain response [7]. In ASR-damaged concrete, the elastic modulus decreases, while the stress-strain hysteresis loops increase in size and increasing amounts of plastic strain accumulate during the course of the test [7,8]. Chrisp et al placed emphasis on the elastic modulus, plastic strain and size of the hysteresis loops of the second through fifth cycles and largely discarded the data from the first load cycle [8].

Further development of the test method by Smaoui et al resulted in a recommended loading level of 10 MPa and identified the area of the first hysteresis loop and the accumulated plastic strain over all five cycles as the most important parameters [9]. They proposed that a linear relationship between these parameters and expansion could be established using laboratory specimens or core samples extracted from larger specimens of known expansion levels [9,10]. Similar to DRI, concrete made with different reactive aggregates will exhibit varying responses in the stiffness damage test; that is, linear relationships must be established for multiple reactive aggregate types in order to estimate the expansion of a variety of field structures [9]. Smaoui et al also proposed shortening the L/D ratio of the test specimens from 2.5 to 2.0 [8,9]. An L/D of 2.0 is a more reasonable value for drilled core specimens and consistent with standard test cylinder sizes.

This paper presents the results of tests to establish relationships for SDT parameters versus expansion for four reactive aggregates. Both cylinders cast and stored under laboratory conditions and cores extracted from outdoor exposure blocks were used. The effects of ASR on the elastic modulus and compressive strength of the specimens were also explored.

2 MATERIALS AND METHODS

2.1 Overview of Test Specimens

Two sets of concrete cylinders (100 x 200 mm) and two sets of four unreinforced concrete outdoor exposure blocks (380 x 380 x 710 mm) were prepared for this study, using four reactive aggregates from the southwestern United States. From each set of cylinders, three were instrumented for axial expansion measurements with stainless steel gage studs. The remaining cylinders in each set were assumed to have expanded the same as the average of the three reference cylinders. The outdoor exposure blocks were instrumented with embedded stainless steel rods with machined divots to allow expansion measurements with DEMEC gauges along on all faces except for the bottoms of the blocks. Expansions were measured in the longitudinal (500 mm gauge length) and transverse (150 mm gauge length) directions on the tops of the blocks, the longitudinal direction (500 mm gauge length) on the front and back faces, and the vertical direction (150 mm gauge length) on the left and right faces. At increasing expansion levels, core samples (95 to 102 mm diameter) were extracted for a suite of tests; three cores from each block were designated for the mechanical tests presented in this study.

2.2 Materials and mixture proportions

The reactive aggregates used in the concrete cylinders were a highly-reactive natural sand from El Paso, Texas (El Paso) and a highly-reactive mixed gravel from Bernalillo, New Mexico (New Mexico). Both contain many particles of volcanic origin. These aggregates were also included in work by Smaoui et al [9]. For the exposure blocks, a highly-reactive natural sand from Robstown, Texas (Robstown) and a moderately-reactive gravel from the Rio Grande valley near Eagle Pass, Texas were used. Each reactive aggregate was paired with a non-reactive crushed stone or manufactured sand from San Antonio, Texas. All aggregates

were delivered in bulk directly from the producer and randomly sampled from the delivered stockpile. For the cylinders, the coarse aggregates were sieved and graded as specified in ASTM C1293 [11]. Aggregates were used as-received for the exposure blocks.

Each set of cylinders was cast from a single batch, while each exposure block was cast from a separate batch of concrete. High-alkali Type I cement was used, and NaOH was added to each batch for a total Na_2O_e of 5.25 kg/m^3 (1.25% by mass of cement). Due to the mild winters in Austin, Texas, no air entrainment was required for the outdoor exposure blocks. Table 1 shows the mixture proportions for all specimens. Concrete was mixed and placed in accordance with ASTM C192; the exposure block concrete was also placed and consolidated in two equal layers [12].

2.3 Conditioning and Monitoring of Specimens

Cylinders

The cylinders were moist-cured for 24 h at 23°C and demolded. The gauge studs were then epoxied into 13.5 mm-deep holes drilled in each end of the reference cylinders, providing an axial gauge length of 173 mm. The cylinders were wrapped in plastic to prevent moisture loss while the epoxy set. Initial length measurements were then recorded with a 0.001 mm-precision dial gage and all cylinders were then stored above water at 38°C and $>95\%$ RH.

All cylinders were kept in the same storage conditions; thus, when reference cylinders were cooled to 23°C for expansion measurements, all cylinders in the set were also moved to the same 23°C environmental chamber. Expansion measurements were initially taken weekly, and then less frequently as the rate of expansion slowed. Figure 1 shows the average expansion of the reference cylinders with time. The New Mexico specimens were cast later and therefore less test data is available. At increasing levels of expansion, three non-instrumented cylinders were selected for mechanical testing. The specimens were either capped with sulphur compound or ground plane with a diamond grinder in preparation for testing.

Core Specimens

Exposure blocks were moist cured at 23°C for seven days. Initial expansion measurements were taken and the blocks moved to an outdoor exposure site in Austin, Texas, where they were subjected to ambient conditions. Expansion measurements were taken only when temperatures were 23°C ($\pm 2^\circ\text{C}$) and cloudy skies to minimize environmental effects. Figure 2 shows the average expansions of the exposure blocks with time, up to the time they were selected for core extraction.

At increasing levels of expansion, a set of core specimens was extracted from a block for testing (three blocks were cored from each set, with the fourth allowed to continue expanding). The cores were cut to length ($200 \pm 3 \text{ mm}$) wrapped and stored in sealed buckets after extraction until testing. Prior to testing, cores were placed in a 23°C and 100% RH chamber for up to two days (less than 0.1% mass change in 24 h) so that all cores were similarly saturated with moisture at testing. Specimens were then either capped with sulphur compound or ground plane with a diamond grinder in preparation for testing.

2.4 Test Procedures

The core or cylinder was placed in a compressometer described by ASTM C469 [13] and subjected to five load cycles with an MTS closed-loop hydraulic testing machine. A loading and unloading rate of 0.1 MPa/s was applied, with a peak compressive stress of 10 MPa. An LVDT mounted in the compressometer provided specimen deformation data, while the MTS controller recorded the applied load. Data was sampled four times per second. The load-deformation data was used to calculate and plot the stress-strain curve for

each specimen. The area of the first load cycle hysteresis loop was calculated by subtracting the area under the unloading curve from the area under the loading curve.

Following the stiffness damage test, the static secant modulus of elasticity and compressive strength of the specimens were determined, in accordance with ASTM C39, C42 and C469 [13,14,15]. The estimated compressive strength was used to determine the applied load for the elastic modulus test, which was then verified by the compressive strength test. The actual applied load varied from 0.31 to 0.43 f_c for the cylinders and 0.33 to 0.41 f_c for the core specimens. Secant moduli should be nearly identical for peak loads of 0.30 to 0.45 f_c ; the loads used in this study are well within that range [16].

3 RESULTS

Tables 2 and 3 summarize the stiffness damage test data for the individual cylinders and cores, respectively. For both the cylinders and cores, the area of the first load cycle had a lower coefficient of variation than the plastic strain over all five cycles. Figure 3 shows the stress-strain data from tests of six El Paso cylinders at increasing levels of expansion. The size of the hysteresis loops clearly increase with expansion, with the exception of the final specimen. The decreasing stiffness and general increase in plastic strain with expansion is also evident.

Figure 4 shows the average stiffness damage test data for the cylinder specimens. Figure 5 shows the average stiffness damage test data for the core specimens. A linear best-fit line and R^2 value is also shown for each plot in Figures 4 and 5. The R^2 value of the best-fit line for the first cycle area varied from 0.39 for the Robstown cores to 1.00 for the Eagle Pass cores; in the plastic strain plots, the R^2 value ranged from 0.27 for the Robstown cores to 0.77 for the El Paso cylinders. The coefficients of variation for plastic strain averaged 23.7% and 24.0% for each set of cylinders and cores, respectively. The first cycle area data was much more consistent, with coefficients of variation averaging 11.8% and 17.7% for each set of cylinders and cores, respectively.

Tables 4 and 5 summarize the elastic modulus and compressive strength data for the individual cylinders and cores, respectively. The elastic modulus is also compared to that which is commonly assumed from the compressive strength ($E = 4700\sqrt{f'_c}$). Undamaged specimens typically exhibited elastic moduli near this assumed value, based on their compressive strengths; however increasing levels of expansion resulted in moduli well below that which would be predicted by compressive strength. The El Paso cylinders at 0.379% expansion had a measured elastic modulus of 51.9% of the value calculated by compressive strength. The coefficients of variation for compressive strength was the lowest of all four parameters examined in this study, averaging 2.7% and 5.3% for each set of cylinders and cores, respectively. The elastic modulus data was also more consistent than the two stiffness damage parameters; the coefficients of variation averaged 5.0% and 9.0% for each set of cylinders and cores, respectively.

4 DISCUSSION

The results suggests there are significant difficulties with the use of the stiffness damage test, as described here, to estimate the expansion of concrete affected by ASR. The test fails to produce consistent results; this is best seen when examining the results of the cylinder specimens, which were produced in a single batch per aggregate type and stored in controlled conditions. The core specimens, however, were removed from exposure blocks that had been stored outdoors in uncontrolled climatic conditions and often experienced local variations in amount of expansion; thus, they would be expected to have a higher coefficient of variation. The coefficients of variation were high, and particularly so for the plastic strain data (an average of 23.7% for the cylinders, but as much as 44.1%). The test also loads specimens to a variable percentage of the compressive strength, as the peak load of 10 MPa is fixed. In this study, the peak load

ranged from 20.6 to 34.6% of the compressive strength for all specimens. Finally, the stiffness damage parameters varied widely in their ability to produce a usable linear relationship with expansion. This may be related, in part, to the fact that the peak load did not represent a consistent percentage of the compressive strength. Only the first cycle area data for the Eagle Pass cores produced an excellent fit to a linear relationship. For all other aggregate and stiffness damage parameter combinations tested, it is difficult to justify the use of a linear best-fit to estimate expansion to date.

The compressive strength and elastic modulus data were significantly more consistent. Although they do not result in a linear relationship with expansion, they do provide information that is potentially useful for structural assessment. The coefficients of variation for both tests were much lower and were within, or very close to, that recommended for tests of undamaged concrete [13, 14]. The data also confirm what has been reported in the literature – that compressive strength and elastic modulus are affected at different rates due to ASR. Therefore, in assessing concrete affected by ASR, the elastic modulus of core specimens should be measured directly, rather than derived from compressive strength tests.

Aging of the ASR gel in the various specimens in this study is likely to have contributed to some of the difficulty in establishing useful relationships of strength, elastic modulus, or stiffness damage parameters to specific levels of expansion. Swamy [3] suggested that as ASR aged and become less fluid, it would contribute to a recovery of the mechanical properties of the affected concrete. This data for the El Paso cylinders is particularly supportive of this hypothesis. The final two sets of specimens were tested at 140 and 273 days of age at expansions of 0.379 and 0.416%, respectively; expansion had slowed significantly, while the cylinders showed a universal improvement in mechanical properties and stiffness damage parameters. Since ASR generally takes place over a much longer timeframe than these accelerated tests, it is possible that aging of the gel will have an even greater impact.

5 CONCLUSIONS

In this study, concrete cylinders and core specimens drilled from plain concrete exposure blocks were subjected to a suite of mechanical tests. This included the stiffness damage test (to 10 MPa peak load), static secant modulus of elasticity, and compressive strength, in that order. From this study, the following conclusions can be drawn:

- Both the area of the first load cycle and the total accumulated plastic strain in the stiffness damage test generally increase with higher levels of expansion from ASR. However, the degree to which each stiffness damage parameter can be fit to a linear relationship with expansion varies for each aggregate.
- With the exception of the first-cycle area data for the Eagle Pass core specimens, the stiffness damage data examined in this study can not be characterized as increasing linearly with expansion.
- Elastic modulus and compressive strength generally decreased with increasing expansion, but at different rates. For this reason, elastic modulus should be measured directly, rather than derived from compressive strength tests on a core specimen.
- The elastic modulus and compressive strength tests produced significantly more consistent results than the stiffness damage test.
- Recovery of mechanical properties may occur with time, even at high levels of expansion, and complicate attempts to relate changes in these properties to specific levels of expansion from ASR.

6 REFERENCES

- [1] ISE. *Structural Effects of Alkali-Silica Reaction*. London: The Institution of Structural Engineers, SETO, 1992, 45.

- [2] Ahmed, T., E. Burley, S. Rigden, and A.I. Abu-Tair. "The Effect of Alkali Reactivity on the Mechanical Properties of Concrete." *Construction and Building Materials* 17 (2003): 123-144.
- [3] Swamy, R N. "Assessment and Rehabilitation of AAR-affected Structures." *Cement and Concrete Composites* 19, no. 5-6 (1997): 427-440.
- [4] Grattan-Bellew, P.E. "Laboratory Evaluation of Alkali-Silica Reaction in Concrete from Saunders Generating Station." *ACI Materials Journal* 95 (March-April 1995): 126-134.
- [5] Rivard, P, B Fournier, and G Ballivy. "Quantitative Assessment of Concrete Damage Due to Alkali-Silica Reaction (ASR) by Petrographic Analysis." Edited by M-A Bérubé, B Fournier and B Durand. *Proceedings of the 11th International Conference on Alkali-Aggregate Reaction*. Québec City, 2000. 889-898.
- [6] Rivard, P., and G. Ballivy. "Assessment of the expansion related to alkali-silica reaction by the Damage Rating Index method." *Construction and Building Materials* 19, no. 2 (March 2005): 83-90.
- [7] Crouch, R S, and J G M Wood. "Damage Evolution in AAR Affected Structures." *International Symposium on Fracture Damage of Concrete and Rock*. Vienna, July 1988.
- [8] Chrisp, T M, P Waldron, and J G M Wood. "Development of a Non-destructive Test to Quantify Damage in Deteriorated Concrete." *Magazine of Concrete Research* 45, no. 165 (1993): 247-256.
- [9] Smaoui, Nizar, Marc-Andre Berube, Benoit Fournier, Benoit Bissonette, and Benoit Durand. "Evaluation of the expansion attained to date by concrete affected by alkali silica reaction. Part I: Experimental study." *Canadian Journal of Civil Engineering* 31, no. 5 (2004): 826-845.
- [10] Smaoui, N, B Fournier, M-A Bérubé, B Bissonette, and B Durand. "Evaluation of the Expansion Attained to Date by Concrete Affected by Alkali-Silica Reaction. Part II: Application to Nonreinforced Concrete Specimens Exposed Outside." *Canadian Journal of Civil Engineering* 31, no. 6 (2004): 997-1011.
- [11] ASTM C 1293-08b. "Standard Test Method for Determination of Length Change of Concrete Due to Alkali-Silica Reaction." West Conshohocken, PA, United States: ASTM International, 2008.
- [12] ASTM C 192-07. "Standard Practice for Making and Curing Concrete Test Specimens in the Laboratory." West Conshohocken, PA: ASTM International, 2007.
- [13] ASTM C 469-10. "Standard Test Method for Static Modulus of Elasticity and Poisson's Ratio of Concrete in Compression." West Conshohocken, Pennsylvania: ASTM International, 2010.
- [14] ASTM C 39-10. "Standard Test Method for Compressive Strength of Cylindrical Concrete Specimens." West Conshohocken, Pennsylvania: ASTM International, 2010.
- [15] ASTM C 42-11. "Standard Test Method for Obtaining and Testing Drilled Cores and Sawed Beams of Concrete." West Conshohocken, Pennsylvania: ASTM International, 2011.
- [16] Popovics, S. *Strength and Related Properties of Concrete: A Quantitative Approach*. New York: John Wiley & Sons, 1998.

Component	El Paso Sand	New Mexico Gravel	Robstown Sand	Eagle Pass Gravel
Coarse Aggregate (kg/m ³)	Crushed limestone; non-reactive 1107	Mixed gravel; highly reactive 1161	Crushed limestone; non-reactive 1107	River gravel; moderately reactive 1203
Fine Aggregate (kg/m ³)	Natural sand; highly reactive 626	Manufactured sand; non-reactive 561	Natural sand; highly reactive 621	Manufactured sand; non-reactive 525
Cement (kg/m ³)	420	420	420	420
(wt% Na ₂ O _e)	0.90	0.90	0.83	0.83
Total Na ₂ O _e (kg/m ³)	5.25	5.25	5.25	5.25
NaOH added	1.90	1.90	2.28	2.28
Water (w/cm = 0.42)	176	176	176	176

		El Paso Sand						New Mexico Gravel			
		Expansion Level (%)						Expansion Level (%)			
		0.009	0.109	0.181	0.272	0.379	0.416	0.010	0.045	0.074	0.135
1st Cycle Area (Pa)	Cyl 1	362	1251	1457	2140	2408	1662	422	753	674	632
	Cyl 2	278	1022	1128	1830	2254	1428	481	648	742	831
	Cyl 3	383	979	1178	1845	2110	1640	339	766	615	661
	<i>Average</i>	<i>341</i>	<i>1084</i>	<i>1254</i>	<i>1938</i>	<i>2257</i>	<i>1577</i>	<i>414</i>	<i>722</i>	<i>677</i>	<i>708</i>
	<i>CV %</i>	<i>16.3</i>	<i>13.5</i>	<i>14.1</i>	<i>9.0</i>	<i>6.6</i>	<i>8.2</i>	<i>17.2</i>	<i>9.0</i>	<i>9.4</i>	<i>15.2</i>
Plastic Strain ($\mu\text{m}/\text{m}$)	Cyl 1	62	179	194	236	270	200	45	92	77	62
	Cyl 2	53	111	119	196	226	153	61	62	97	125
	Cyl 3	46	113	108	226	217	206	23	61	92	65
	<i>Average</i>	<i>54</i>	<i>134</i>	<i>140</i>	<i>220</i>	<i>238</i>	<i>186</i>	<i>43</i>	<i>71</i>	<i>89</i>	<i>84</i>
	<i>CV %</i>	<i>14.7</i>	<i>28.9</i>	<i>33.4</i>	<i>9.5</i>	<i>11.9</i>	<i>15.7</i>	<i>44.1</i>	<i>25.0</i>	<i>11.4</i>	<i>42.1</i>
f_c (28 day)		37.8						37.2			
Load, % of 28-day f_c		26.4						26.9			
Load, % of f_c at test		29.5	28.3	30.1	32.7	34.6	34.0	27.9	27.3	26.4	25.2

		Robstown Sand			Eagle Pass Gravel		
		Expansion Level (%)			Expansion Level (%)		
		0.082	0.172	0.354	0.075	0.119	0.177
1st Cycle Area (Pa)	Core 1	371	1133	928	n/a	984	1322
	Core 2	412	766	862	615	989	810
	Core 3	466	959	767	763	595	1044
	<i>Average</i>	<i>416</i>	<i>953</i>	<i>852</i>	<i>689</i>	<i>856</i>	<i>1059</i>
	<i>CV %</i>	<i>11.4</i>	<i>19.3</i>	<i>9.5</i>	<i>15.2</i>	<i>26.4</i>	<i>24.2</i>
Plastic Strain ($\mu\text{m}/\text{m}$)	Core 1	48	131	108	n/a	121	144
	Core 2	45	88	98	84	27	87
	Core 3	54	127	79	92	65	131
	<i>Average</i>	<i>49</i>	<i>115</i>	<i>95</i>	<i>88</i>	<i>71</i>	<i>121</i>
	<i>CV %</i>	<i>9.9</i>	<i>20.3</i>	<i>15.6</i>	<i>6.8</i>	<i>66.8</i>	<i>24.7</i>
f_c (28 day)		46.4	45.0	45.6	36.1	33.3	35.6
Load, % of 28-day f_c		21.5	22.2	21.9	27.7	30.0	28.1
Load, % of f_c at test		20.6	21.2	25.8	27.0	30.2	33.6

		El Paso Sand						New Mexico Gravel			
		Expansion Level (%)						Expansion Level (%)			
		0.009	0.109	0.181	0.272	0.379	0.416	0.010	0.045	0.074	0.135
E (GPa)	Cyl 1	27.9	20.0	17.6	13.4	13.0	15.8	29.5	26.3	24.3	23.5
	Cyl 2	29.2	21.2	19.3	15.5	12.4	16.7	30.3	25.6	23.9	22.7
	Cyl 3	30.2	19.0	16.6	15.7	13.8	15.4	29.0	25.2	25.6	25.6
	<i>Average</i>	<i>29.1</i>	<i>20.1</i>	<i>17.9</i>	<i>14.9</i>	<i>13.1</i>	<i>16.0</i>	<i>29.6</i>	<i>25.7</i>	<i>24.6</i>	<i>23.9</i>
	<i>CV %</i>	<i>4.0</i>	<i>5.5</i>	<i>7.7</i>	<i>8.5</i>	<i>5.7</i>	<i>4.0</i>	<i>2.3</i>	<i>2.2</i>	<i>3.8</i>	<i>6.3</i>
f _c (MPa)	Cyl 1	33.0	35.2	32.2	30.1	28.7	28.9	35.4	36.0	35.3	39.9
	Cyl 2	33.8	34.6	34.8	30.4	29.3	29.6	36.8	37.2	41.5	39.2
	Cyl 3	34.9	36.3	32.8	31.1	28.7	29.6	35.4	36.7	37.1	40.0
	<i>Average</i>	<i>33.9</i>	<i>35.4</i>	<i>33.3</i>	<i>30.6</i>	<i>28.9</i>	<i>29.4</i>	<i>35.9</i>	<i>36.6</i>	<i>37.9</i>	<i>39.7</i>
	<i>CV %</i>	<i>2.7</i>	<i>2.3</i>	<i>4.2</i>	<i>1.7</i>	<i>1.2</i>	<i>1.3</i>	<i>2.3</i>	<i>1.6</i>	<i>8.4</i>	<i>1.0</i>
E _s % of predicted by f _c		105.6	71.3	65.4	56.9	51.3	62.3	104.5	89.7	84.5	80.1

		Robstown Sand			Eagle Pass Gravel		
		Expansion Level (%)			Expansion Level (%)		
		0.082	0.172	0.354	0.075	0.119	0.177
E (GPa)	Core 1	25.3	22.4	18.1	29.0	20.9	19.2
	Core 2	25.1	24.4	18.7	23.8	22.6	24.0
	Core 3	26.3	21.5	20.8	19.8	23.4	19.7
	<i>Average</i>	<i>25.6</i>	<i>22.8</i>	<i>19.2</i>	<i>24.2</i>	<i>22.3</i>	<i>21.0</i>
	<i>CV %</i>	<i>2.7</i>	<i>6.6</i>	<i>7.4</i>	<i>19.1</i>	<i>5.6</i>	<i>12.5</i>
f _c (MPa)	Core 1	48.1	45.9	37.9	38.6	29.7	31.6
	Core 2	49.3	48.4	38.8	37.5	33.6	31.8
	Core 3	48.4	47.4	39.4	34.9	36.0	25.8
	<i>Average</i>	<i>48.6</i>	<i>47.3</i>	<i>38.7</i>	<i>37.0</i>	<i>33.1</i>	<i>29.7</i>
	<i>CV %</i>	<i>1.3</i>	<i>2.7</i>	<i>1.9</i>	<i>5.1</i>	<i>9.6</i>	<i>11.4</i>
E _s % of predicted by f _c		77.4	70.0	65.0	83.8	81.9	81.3

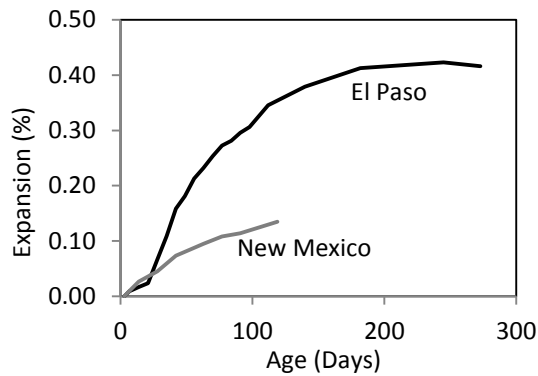


Figure 1. Average expansions of El Paso and New Mexico reference cylinders.

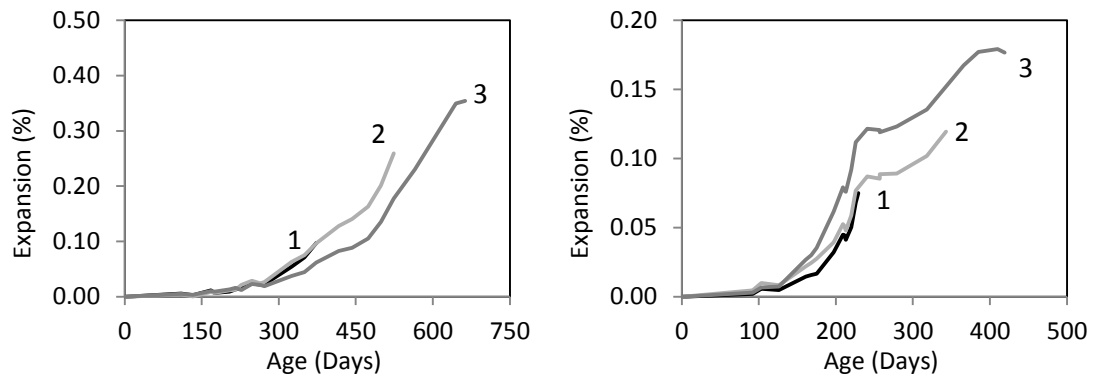


Figure 2. Average expansions of Robstown (left) and New Mexico (right) exposure blocks.

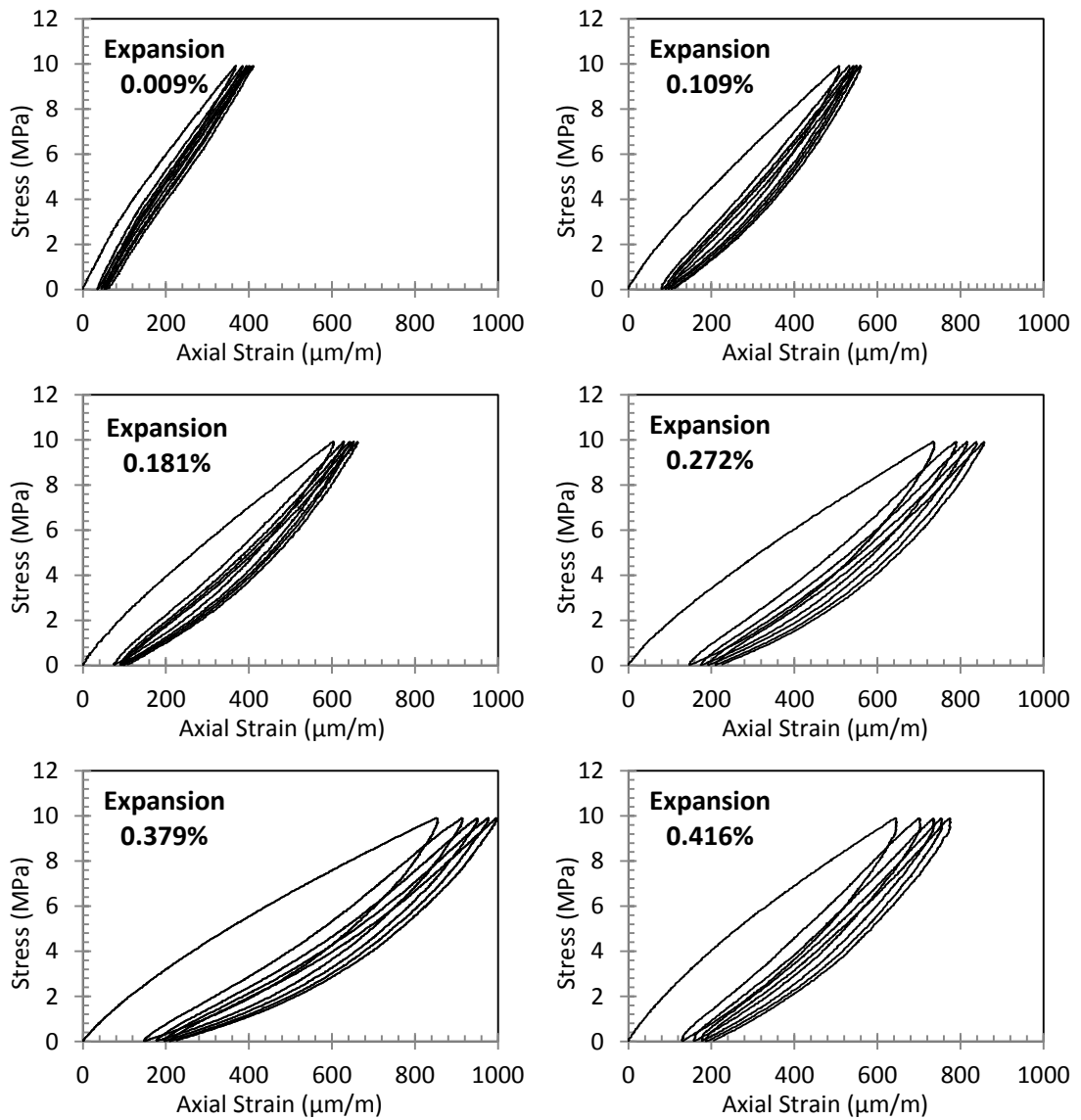


Figure 3: Stiffness damage test stress-strain plots for selected El Paso cylinders.

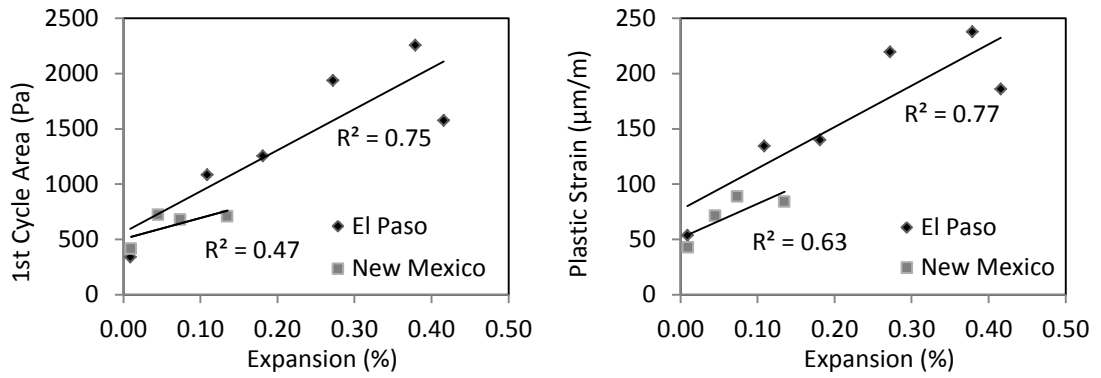


Figure 4: SDT data for cylinders (each datum is average of 3 cylinders).

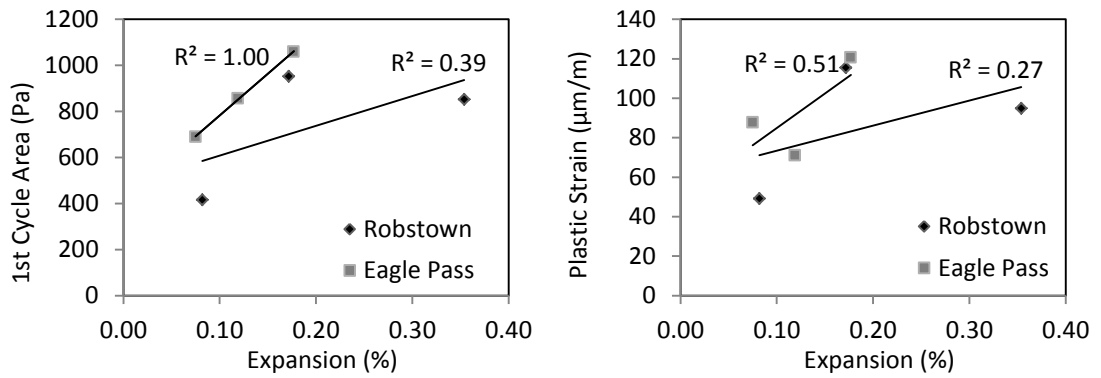


Figure 5: SDT data for core specimens (each datum is average for that expansion level).